Optimal implementation of two-qubit linear-optical quantum filters

Jaromír Fiurášek, Robert Stárek, and Michal Mičuda
Department of Optics, Palacký University, 17. listopadu 1192/12, 771 46 Olomouc, Czech Republic

(Received 26 February 2021; accepted 19 May 2021; published 7 June 2021)

We design optimal interferometric schemes for the implementation of two-qubit linear-optical quantum filters diagonal in the computational basis. The filtering is realized by the interference of the two photons encoding the qubits in a multiport linear-optical interferometer, followed by conditioning on presence of a single photon in each output port of the filter. The filter thus operates in the coincidence basis, similarly to many linear-optical unitary quantum gates. The implementation of a filter with linear optics may require an additional overhead in terms of a reduced overall success probability of the filtering and the optimal filters are those that maximize the overall success probability. We discuss in detail the case of symmetric real filters and extend our analysis also to asymmetric and complex filters.

DOI: 10.1103/PhysRevA.103.062408

I. INTRODUCTION

Quantum information processing with linear optics [1–3] relies on the encoding of qubits into states of single photons and the implementation of various quantum operations by multiphoton interference, followed by photon counting measurements and postselection based on the measurement outcomes. Scalable linear-optical quantum gates can be in principle realized with the use of auxiliary single photons and feedforward operations controlled by the outcomes of measurements on auxiliary modes [4,5]. During the past two decades, quantum information processing with linear optics has evolved rapidly, driven in recent years by important advances in the design of integrated quantum optics circuits on a chip [6], and highly efficient superconducting single-photon detectors [7,8] and single-photon sources [9,10]. Although full-scale quantum computing with linear optics still appears to be technologically very demanding, the linear-optics platform proved to be very useful for proof-of-principle tests of various concepts and protocols in quantum information processing, and small-scale linear-optical quantum processors may find their applications in advanced quantum communication networks, where the role of light as the information carrier is indispensable.

A central topic in quantum computing with linear optics is to design and realize various two-qubit [5] and multiqubit [11–15] linear-optical quantum gates. Besides unitary gates, nonunitary quantum operations, commonly referred to as quantum filters, also play an essential role in quantum information processing. A quantum filter can be defined as a trace-decreasing completely positive map with a single Kraus operator M that satisfies $M^\dagger M \leqslant I$ and transforms a general input state $\rho_{\rm in}$ as $\rho_{\rm out} = M\rho_{\rm in}M^\dagger$. This output state is not normalized and $P_S = {\rm Tr}[\rho_{\rm out}]$ is the probability of successful filtering. Quantum filters find their applications for instance in optimal quantum state discrimination [16,17], entanglement concentration and distillation [18–21], or in the engineering of highly nonclassical states of light by conditional photon addition or subtraction [22–26].

In the present work we investigate the optimal linear-optical implementation of a two-qubit quantum filter diagonal in the computational basis,

$$M = m_{00}|00\rangle\langle 00| + m_{01}|01\rangle\langle 01| + m_{10}|10\rangle\langle 10| + |11\rangle\langle 11|, \tag{1}$$

where $|m_{jk}| \leqslant 1$, and without loss of generality we set $m_{11} = 1$. We concentrate on the resource-effective implementation that does not require any auxiliary photons. The filter is realized by the interference of the two photons encoding the qubits in a suitably designed multiport optical interferometer, and successful filtering is heralded by the presence of a single photon in each output of the filter. The filter thus operates in the coincidence basis, similarly to a number of linear-optical unitary quantum gates designed and realized to date. In practice, the verification of the presence of a single photon in each output of the filter would require destructive coincidence two-photon detection. The quantum filters M can be considered as a generalization of two-qubit controlled-phase gates, where phase modulation is replaced by amplitude modulation. Specifically, for $m_{00} = 1$ and $m_{01} = m_{10} = 0$ the filter (1) becomes the quantum parity check [27–29] that is useful for implementation of a linear-optical controlled-NOT (CNOT) gate [28,30,31] and for the generation of entangled multiphoton cluster states [32].

It turns out that, depending on the filter parameters, it may not be possible to implement the filter without an additional reduction of the probability of success. This means that instead of filter M we implement an equivalent but less efficient filter $\sqrt{P_L}M$, where P_L is the probability reduction factor imposed by the linear-optical setup. Our goal is to design optimal interferometric schemes for the two-qubit quantum filters (1), that maximize the probability P_L. This task is similar to the design of optimal two-qubit linear-optical phase gates operating in the coincidence basis [33,34]. However, in contrast

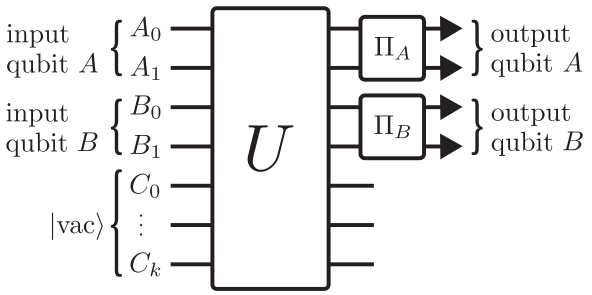

FIG. 1. Two-qubit linear-optical quantum filter operating in the coincidence basis. Qubits are encoded into states of single photons in pairs of modes A_0, A_1 and B_0, B_1. The scheme involves also auxiliary input modes C_j that are all prepared in a vacuum state. All modes are coupled in a multiport optical interferometer described by a unitary matrix U. The filter is conditionally implemented if each pair of output modes A_0, A_1 and B_0, B_1 contains a single photon, and this conditioning is represented in the figure by projectors Π_A and Π_B onto the two-dimensional single-photon subspaces of the respective pairs of modes. In practice, confirmation of a successful filter operation can be achieved in a destructive manner by conditioning on the coincidence detection of two photons, one in modes A_0, A_1, the other in modes B_0, B_1.

to the optimal controlled-phase gate, we find that different mode-coupling configurations are optimal depending on the filter parameters. Importantly, fully analytical results can be obtained for the optimal interferometer parameters and the resulting maximum success probability P_L.

The rest of the paper is organized as follows. In Sec. II we present a general description of the linear-optical interferometric scheme that implements the two-qubit quantum filters. In Sec. III we discuss in detail the realization of a symmetric filter with real coefficients and in Sec. IV we extend our analysis to asymmetric and complex filters. Finally, Sec. V contains a brief summary and conclusions. The Appendix contains technical proof of the allowed structure of the interferometer that implements the quantum filter.

II. LINEAR-OPTICAL TWO-QUBIT QUANTUM FILTERS

A conceptual scheme of a linear-optical setup implementing the two-qubit quantum filter (1) is depicted in Fig. 1. Each qubit is encoded into the state of a single photon that can propagate in two modes denoted as A_0, A_1, and B_0, B_1 for qubits A and B, respectively. The presence of a photon in mode A_0, B_0 represents a logical state $|0\rangle$ while a photon in mode A_1, B_1 encodes a logical state $|1\rangle$. The quantum filter is implemented by the interference of the two photons in a multiport optical interferometer followed by verification of the presence of a single photon in each pair of output modes A_0, A_1 and B_0, B_1. In practice, this verification can be performed destructively by conditioning on suitable two-photon coincidence detection. The linear-optical quantum filter thus operates in the coincidence basis, similarly to certain linear-optical two-qubit CNOT and controlled-phase gates [5,35–37]. This approach is applicable in practice provided that the quantum filter represents the last operation on the qubits before their detection at the output of the optical quantum information processing network.

Alternatively, one can perform a nondemolition detection of a single photon in each pair of modes. However, within the linear-optics setting, this would require ancilla photons [38] and would significantly increase the complexity of the filter and reduce its success rate. Alternatively, the nondestructive implementation of a two-qubit quantum filter with ancilla photons may be also achieved by imprinting the filter into an ancilla two-photon entangled state, similarly to implementations of a nondestructive two-qubit linear-optical CNOT gate [30,31].

A multiport optical interferometer can be described by a unitary matrix U that specifies the coupling between the input and output modes. Note that in addition to the four modes that encode the qubits, the interferometer may contain also additional auxiliary modes. In terms of creation operators $c_j^\dagger$ associated with each mode we have

$$c_{j,\text{in}}^\dagger = \sum_k U_{j,k} c_{k,\text{out}}^\dagger. \tag{2}$$

Throughout the paper we use a boldface font for the Fock states and a lightface font for the logical qubit basis states. Let

$$|\mathbf{1}_{A_j}, \mathbf{1}_{B_k}\rangle = c_{A_j}^\dagger c_{B_k}^\dagger |\text{vac}\rangle, \tag{3}$$

where $j, k \in \{0, 1\}$ and $|\text{vac}\rangle$ is the vacuum state, denote the input two-photon Fock state corresponding to the two-qubit product state $|j\rangle_A |k\rangle_B$. The projectors Π_A and Π_B on two-mode single-photon subspaces indicated in Fig. 1 can be expressed as

$$\begin{aligned}\Pi_A &= |\mathbf{1}_{A_0}, \mathbf{0}_{A_1}\rangle\langle \mathbf{1}_{A_0}, \mathbf{0}_{A_1}| + |\mathbf{0}_{A_0}, \mathbf{1}_{A_1}\rangle\langle \mathbf{0}_{A_0}, \mathbf{1}_{A_1}|,\\ \Pi_B &= |\mathbf{1}_{B_0}, \mathbf{0}_{B_1}\rangle\langle \mathbf{1}_{B_0}, \mathbf{0}_{B_1}| + |\mathbf{0}_{B_0}, \mathbf{1}_{B_1}\rangle\langle \mathbf{0}_{B_0}, \mathbf{1}_{B_1}|.\end{aligned} \tag{4}$$

Conditional on the observation of a single photon in each pair of output modes A_0, A_1 and B_0, B_1, the input two-photon Fock state (3) transforms according to

$$|\mathbf{1}_{A_j}, \mathbf{1}_{B_k}\rangle \to \sum_{m,n=0}^{1} W_{A_m,B_n|A_j,B_k} |\mathbf{1}_{A_m}, \mathbf{1}_{B_n}\rangle, \tag{5}$$

where

$$W_{A_m,B_n|A_j,B_k} = U_{A_j,A_m} U_{B_k,B_n} + U_{A_j,B_n} U_{B_k,A_m}. \tag{6}$$

Correct implementation of the quantum filter (1) requires that

$$W_{A_m,B_n|A_j,B_k} = \sqrt{P_L} m_{jk} \delta_{jm} \delta_{kn}, \tag{7}$$

where $P_L \leqslant 1$ is an additional factor that may reduce the overall probability of implementation of the linear-optical quantum filter. Our goal is to find for a given filter (1) the optimal interferometer that maximizes P_L.

The design of optimal linear-optical quantum filters is similar to the construction of an optimal linear-optical two-qubit quantum controlled-phase gate operating in the coincidence basis [33,34]. In particular, one can show that correct functioning of the two-qubit quantum filter as specified by Eq. (7) can be achieved only if only one pair of information-encoding modes is interferometrically coupled (see the Appendix for a proof). Consequently, the 4×4 matrix $U_{AB} = (U_{j,k})$, where $j, k \in \{A_0, B_0, A_1, B_1\}$, has a block-diagonal structure, consisting of a general 2×2 matrix describing the coupling of

two modes and two additional diagonal elements specifying the amplitude transmittances for the other two modes. For an explicit example of such matrix, see, e.g., Eq. (10) below. In what follows, we will frequently use the conditions under which a 2×2 matrix $V = (V_{j,k})$ is a submatrix of a unitary matrix. Define two row vectors $\vec{v}_j = (V_{j,0}, V_{j,1})$. Matrix V is a submatrix of a unitary matrix if and only if the vector norms and scalar product satisfy the inequalities,

$$|\vec{v}_0|^2 \leqslant 1, \quad |\vec{v}_1|^2 \leqslant 1,$$
$$|\vec{v}_0 \cdot \vec{v}_1|^2 \leqslant (1 - |\vec{v}_0|^2)(1 - |\vec{v}_1|^2). \tag{8}$$

Here, the last inequality guarantees that the vectors $\vec{v}_0$ and $\vec{v}_1$ can be completed to orthogonal vectors of unit length.

III. SYMMETRIC REAL FILTER

In this section we investigate the optimal interferometric schemes for the implementation of a two-qubit real symmetric quantum filter specified by the Kraus operator

$$M = a|00\rangle\langle 00| + b(|01\rangle\langle 01| + |10\rangle\langle 10|) + |11\rangle\langle 11|, \tag{9}$$

where $0 \leqslant a \leqslant 1$ and $0 \leqslant b \leqslant 1$. Note that if $a = b^2$, then the filter factorizes and becomes a product of two single-qubit filters that each attenuate the amplitude of the basis state $|0\rangle$ by a factor b. Otherwise, the quantum filter is an entangling operation that can create entangled states from input separable states. When optimizing the success probability P_L, it is necessary to consider three different configurations: the coupling of modes A_0 and B_0, the coupling of modes A_1 and B_1, and finally also the coupling of modes B_0 and A_1. Note that due to the symmetry of the filter, the fourth possible configuration, where modes B_1 and A_0 are coupled, is fully equivalent to the configuration where modes A_1 and B_0 are coupled, and therefore need not be considered separately. In what follows we discuss each of the above listed configurations in detail.

A. Coupling of modes A_0 and B_0

Assuming the coupling of modes A_0 and B_0 and the ordering of modes A_0, B_0, A_1, and B_1, we can write the corresponding 4×4 submatrix of U as follows (see the Appendix),

$$U_{AB} = \begin{pmatrix} \tau_A b & \tau_A x & 0 & 0 \\ \tau_B y & \tau_B b & 0 & 0 \\ 0 & 0 & \tau_A & 0 \\ 0 & 0 & 0 & \tau_B \end{pmatrix}. \tag{10}$$

Here, τ_A and τ_B represent the amplitude attenuation of modes A_1 and B_1, respectively, and the parameters x and y specify the strength of the interferometric coupling between modes A_0 and B_0. Without loss of generality, we can assume that all matrix elements of U_{AB} are real. The parameters x and y are related by the condition

$$xy = a - b^2. \tag{11}$$

The chosen parametrization of the matrix elements of U_{AB} together with the condition (11) ensures that the set of equations (7) is satisfied, where $m_{00} = a$, $m_{01} = m_{10} = b$, $m_{11} = 1$, and

$$P_L = \tau_A^2 \tau_B^2. \tag{12}$$

We are thus left with three free parameters τ_A, τ_B, and x that shall be optimized to maximize the probability P_L.

Since U_{AB} is a submatrix of a unitary matrix, the following constraints must be satisfied [cf. also Eq. (8)],

$$\tau_A^2 \leqslant 1, \quad \tau_B^2 \leqslant 1. \tag{13}$$

$$\tau_A^2(b^2 + x^2) \leqslant 1, \quad \tau_B^2(b^2 + y^2) \leqslant 1, \tag{14}$$

and

$$\tau_A^2 \tau_B^2 b^2 (x + y)^2 \leqslant [1 - \tau_A^2(b^2 + x^2)][1 - \tau_B^2(b^2 + y^2)]. \tag{15}$$

Taking into account the constraint (11), and introducing new parameters z, $\tau_B = z\tau_A$, and $\gamma = |y/x|z$, this last inequality can be rewritten as

$$\sqrt{P_L} b^2 (z^{-1} + z) + \sqrt{P_L}|a - b^2|(\gamma^{-1} + \gamma) - P_L(2b^2 - a)^2 \leqslant 1. \tag{16}$$

Since

$$x + x^{-1} \geqslant 2, \quad \forall x > 0, \tag{17}$$

we get

$$2\sqrt{P_L}(b^2 + |a - b^2|) - P_L(2b^2 - a)^2 \leqslant 1. \tag{18}$$

This inequality yields a nontrivial upper bound on P_L if $a > b^2$. Assuming equality in Eq. (18), and carefully analyzing the two roots of the resulting quadratic equation for $\sqrt{P_L}$,

$$\sqrt{P_L} = \frac{a \pm 2b\sqrt{a - b^2}}{(2b^2 - a)^2} = \frac{1}{(b \mp \sqrt{a - b^2})^2}, \tag{19}$$

we find that P_L is upper bounded by the smaller root, and

$$P_L \leqslant \frac{1}{(b + \sqrt{a - b^2})^4}, \quad a > b^2. \tag{20}$$

Another useful inequality can be obtained by taking the product of the two inequalities (14). We get

$$P_L[b^4 + b^2|b^2 - a|(\mu + \mu^{-1}) + (b^2 - a)^2] \leqslant 1, \tag{21}$$

where $\mu = |x/y|$. With the use of inequality (17) this yields

$$P_L \leqslant \frac{1}{(b^2 + |b^2 - a|)^2}. \tag{22}$$

We now explicitly present the optimal interferometric configurations that are all symmetric, $\tau_A = \tau_B = \tau$ and $x = \pm y$. We have to distinguish four different cases according to the values of the filter parameters a and b.

(i) $a \leqslant b^2$, $2b^2 - a < 1$. As shown in Fig. 2(a), in this case it is optimal to couple the modes A_0 and B_0 on a beam splitter with amplitude transmittance

$$t = \frac{b}{\sqrt{2b^2 - a}}. \tag{23}$$

Subsequently, each of the modes A_0 and B_0 is attenuated with an amplitude factor

$$\nu = \sqrt{2b^2 - a} \tag{24}$$

by sending it through a beam splitter with an amplitude transmittance ν whose auxiliary mode is prepared in a vacuum state. Since we postselect on the presence of a single photon

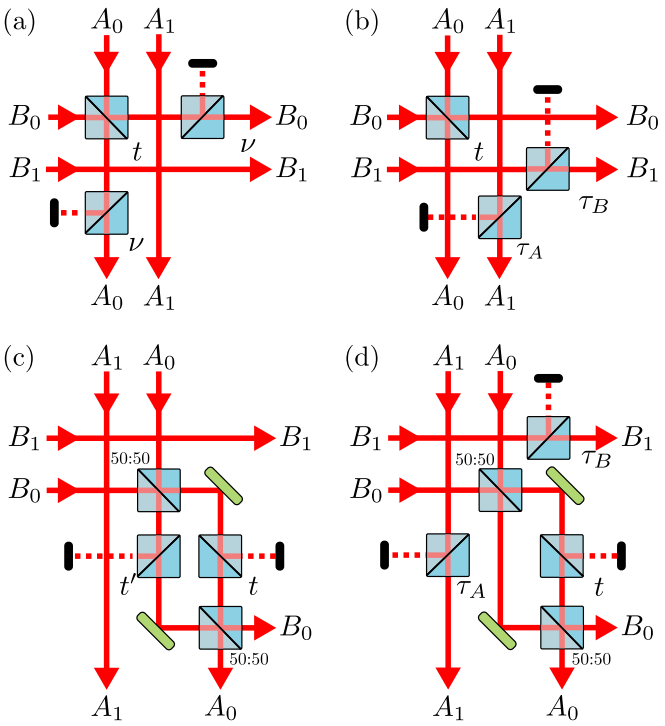

FIG. 2. Optimal optical interferometers implementing the two-qubit quantum filters (9) by the interferometric coupling of modes A_0 and B_0. The labels of the beam splitters indicate their amplitude transmittances. Mode attenuation is realized by propagation through a beam splitter with a suitable transmittance, whose auxiliary input mode is prepared in the vacuum state. The four schemes (a)–(d) represent optimal setups for different values of the filter parameters a and b. For details, see the text.

in each pair of output modes, this mode attenuation only reduces the amplitude of the corresponding Fock state $|\mathbf{1}\rangle$ but it preserves coherence and pure input states are conditionally mapped onto pure output states, as described by Eq. (5). With the setup shown in Fig. 2(a) we get $P_L = 1$ and the linear-optical implementation does not impose any extra reduction of the overall success probability of the quantum filtering.

(ii) $a \leqslant b^2$, $2b^2 - a > 1$. The optimal scheme is drawn in Fig. 2(b) and is similar to that in case (i). However, instead of attenuating modes A_0 and B_0 we have to attenuate modes A_1 and B_1 with amplitude transmittance

$$\tau_A = \tau_B = \frac{1}{\sqrt{2b^2 - a}}. \tag{25}$$

Subsequently, the probability P_L drops below 1 and we get $P_L = (2b^2 - a)^{-2}$. The scheme is optimal because P_L saturates the inequality (22).

(iii) $a > b^2$, $b + \sqrt{a - b^2} \leqslant 1$. The optimal interferometric scheme is shown in Fig. 2(c). Modes A_0 and B_0 are injected into a Mach-Zehnder interferometer formed by two balanced beam splitters. One arm of the interferometer is attenuated with amplitude transmittance t and the other with amplitude transmittance t', where

$$t = b - \sqrt{a - b^2}, \quad t' = b + \sqrt{a - b^2}. \tag{26}$$

In this case we achieve $P_L = 1$.

(iv) $a > b^2$, $b + \sqrt{a - b^2} > 1$. The optimal scheme is shown in Fig. 2(d) and is similar to the scheme for case (iii). However, only one of the interferometer arms is attenuated, with amplitude transmittance

$$t = \frac{b - \sqrt{a - b^2}}{b + \sqrt{a - b^2}}. \tag{27}$$

Furthermore, modes A_1 and B_1 are each attenuated by a factor

$$\tau_A = \tau_B = \frac{1}{b + \sqrt{a - b^2}}. \tag{28}$$

Consequently, we have

$$P_L = \frac{1}{(a + 2b\sqrt{a - b^2})^2}. \tag{29}$$

The scheme is optimal because the achieved P_L saturates the bound (20).

B. Coupling of modes A_1 and B_1

Let us now investigate the configuration where modes A_1 and B_1 are interferometrically coupled instead of the modes A_0 an B_0. Keeping the same ordering of modes A_0, B_0, A_1, and B_1, the relevant 4×4 submatrix of U can be written as

$$U_{AB} = \begin{pmatrix} \tau_A & 0 & 0 & 0 \\ 0 & \tau_B & 0 & 0 \\ 0 & 0 & \frac{b}{a}\tau_A & \tau_A x \\ 0 & 0 & \tau_B y & \frac{b}{a}\tau_B \end{pmatrix}, \tag{30}$$

where

$$xy = \frac{a - b^2}{a^2} \tag{31}$$

and the probability P_L can be expressed as

$$P_L = \frac{\tau_A^2 \tau_B^2}{a^2}. \tag{32}$$

The conditions following from the requirement that (30) is a submatrix of a unitary matrix yield

$$\tau_A^2\left(\frac{b^2}{a^2} + x^2\right) \leqslant 1, \quad \tau_B^2\left(\frac{b^2}{a^2} + y^2\right) \leqslant 1, \tag{33}$$

and

$$2\frac{\sqrt{P_L}}{a}(b^2 + |a - b^2|) - \frac{P_L}{a^2}(2b^2 - a)^2 \leqslant 1. \tag{34}$$

This last inequality was obtained by the same procedure as the inequality (18) and it implies the following upper bound on P_L,

$$P_L \leqslant \frac{a^2}{(b + \sqrt{a - b^2})^4}, \quad a > b^2. \tag{35}$$

By taking the product of the two inequalities (33) and utilizing the constraint (31) we find that

$$P_L \leqslant \frac{a^2}{(b^2 + |b^2 - a|)^2}. \tag{36}$$

For $a < b^2$ this bound is stricter than the bound (22). Similarly, for $a > b^2$ the inequality (35) is stricter than the inequality (20). It follows from the inequalities (35) and (36)

that with the coupling of modes A_1 and B_1 we can achieve $P_L = 1$ only if $a = b^2$. Physically, for $a \neq b^2$ there will always be a nonzero probability that for the input state $|11\rangle$ the two photons will bunch and will both end up either in mode A_1 or B_1, resulting in the failure of the filter. We can therefore conclude that the interferometric coupling of modes A_1 and B_1 cannot yield higher P_L than the coupling of modes A_0 and B_0.

C. Coupling of modes B_0 and A_1

Finally, we consider an asymmetric configuration where modes B_0 and A_1 are coupled. The corresponding matrix U_{AB} can be expressed as

$$U_{AB} = \begin{pmatrix} b\tau_A & 0 & 0 & 0 \\ 0 & \tau_B \frac{a}{b} & \tau_B x & 0 \\ 0 & \tau_A y & \tau_A & 0 \\ 0 & 0 & 0 & \tau_B \end{pmatrix}, \tag{37}$$

where

$$xy = b - \frac{a}{b}. \tag{38}$$

The requirement that U_{AB} is a submatrix of a unitary matrix yields the constraints

$$\tau_A^2(1+y^2) \leqslant 1, \quad \tau_B^2\left(x^2 + \frac{a^2}{b^2}\right) \leqslant 1, \tag{39}$$

and

$$\tau_A^2\tau_B^2\left(x + y\frac{a}{b}\right)^2 \leqslant \left[1 - \tau_A^2(1+y^2)\right]\left[1 - \tau_B^2\left(x^2 + \frac{a^2}{b^2}\right)\right], \tag{40}$$

together with $\tau_A^2 \leqslant 1$ and $\tau_B^2 \leqslant 1$. The optimal schemes must saturate at least one of the inequalities (39) and (40). If none of these inequalities is saturated, then we can increase τ_A, hence also $P_L = \tau_A^2\tau_B^2$, until at least one inequality is saturated.

Let us first assume that one of the inequalities (39) is saturated. It immediately follows from Eq. (40) that $x + ya/b = 0$ must hold, which together with (38) yields

$$x = \frac{1}{b}\sqrt{a(a-b^2)}, \quad y = -\frac{1}{a}\sqrt{a(a-b^2)}. \tag{41}$$

This solution exists in the parameter region $a > b^2$. It follows from the inequalities (39) that the maximum possible values of $\tau_{A,B}$ are given by

$$\tau_A^2 = \frac{a}{2a-b^2}, \quad \tau_B^2 = \min\left(1, \frac{b^2}{a(2a-b^2)}\right). \tag{42}$$

Consequently, the maximum achievable P_L for this case can be expressed as

$$P_L = \min\left(\frac{a}{2a-b^2}, \frac{b^2}{(2a-b^2)^2}\right), \quad a > b^2. \tag{43}$$

Let us now assume that only the inequality (40) is saturated. Since the saturation means that equality holds in (40), we can use it to express τ_A^2 in terms of x and τ_B,

$$\tau_A^2 = \frac{x^2[b^2 - \tau_B^2(b^2x^2 + a^2)]}{x^2b^2 + (b^2-a)^2 - x^2\tau_B^2(2a-b^2)^2}. \tag{44}$$

The optimal values of τ_B and x can be determined by solving the extremal equations

$$\frac{\partial}{\partial\tau_B}\left(\tau_A^2\tau_B^2\right) = 0, \quad \frac{\partial}{\partial x}\left(\tau_A^2\tau_B^2\right) = 0, \tag{45}$$

where τ_A^2 is given by Eq. (44). In the region $a > b^2$ we recover the optimality condition (41). In the region $a < b^2$ we obtain an additional potentially optimal solution

$$x = \frac{\sqrt{a}}{b}\sqrt{b^2-a}, \quad y = \sqrt{\frac{b^2-a}{a}}, \tag{46}$$

and

$$\tau_A^2 = \frac{a}{(\sqrt{b^2-a}+\sqrt{a})^2}, \quad \tau_B^2 = \frac{b^2}{a}\frac{1}{(\sqrt{b^2-a}+\sqrt{a})^2}. \tag{47}$$

Note that this solution is acceptable only if all the inequalities (13) and (39) are satisfied. Additionally, we have to consider also the extremal point $\tau_B^2 = 1$. On inserting this into Eq. (44), we have

$$P_L = \tau_A^2 = \frac{x^2(b^2 - b^2x^2 - a^2)}{x^2b^2 + (b^2-a)^2 - x^2(2a-b^2)^2}. \tag{48}$$

The optimal x maximizing P_L can be found from the extremal equation

$$\frac{\partial P_L}{\partial x} = 0. \tag{49}$$

After some algebra, this yields two roots,

$$x^2 = \frac{(a+b)(a-b^2)}{b(2a+b-b^2)}, \quad P_L = \frac{(a+b)^2}{(2a+b-b^2)^2}, \tag{50}$$

and

$$x^2 = \frac{(b-a)(b^2-a)}{b(b^2+b-2a)}, \quad P_L = \frac{(a-b)^2}{(b^2+b-2a)^2}. \tag{51}$$

We emphasize that formulas (50) or (51) represent valid potential optimal points only if $x^2 \geqslant 0$ and if all the inequalities (13) and (39) are satisfied.

The final maximization of P_L must be performed over all the above considered configurations and all the identified potentially optimal solutions. The maximal P_L, optimized over all the coupling configurations, is plotted in Fig. 3. Remarkably, we find that for a certain range of parameters a and b satisfying $a > b^2$ the asymmetric scheme where modes B_0 and A_1 are coupled outperforms the symmetric scheme where modes A_0 and B_0 are coupled, and achieves higher P_L. This area of parameters where the coupling of modes B_0 and A_1 is optimal is depicted in Fig. 4. We note that the interferometric coupling described by matrix (37) can be realized by the interference of modes B_0 and A_1 in a Mach-Zehneder interferometer formed by two generally unbalanced beam splitters, and the signal in each interferometer arm should be suitably attenuated [cf. Fig. 2(c)]. The splitting ratios of the beam splitters and the attenuation factors can be determined by the singular value decomposition of the matrix U_{AB} [34].

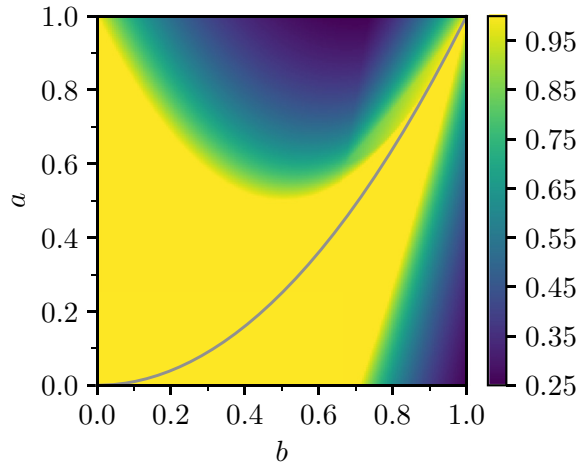

FIG. 3. Maximum probability P_L for the symmetric two-qubit quantum filters (9) achievable with linear-optical interferometric schemes is plotted as a function of filter parameters a and b. The large yellow area represents filters for which $P_L = 1$. The gray line indicates the points $a = b^2$ that correspond to filters which factor into products of single-qubit filters.

IV. ASYMMETRIC AND COMPLEX FILTERS

The optimization procedure discussed in the previous section can be extended to asymmetric and complex two-qubit filters. Here, we illustrate it on the examples of a two-qubit asymmetric filter with real coefficients and a two-qubit symmetric complex filter. We shall focus on the configuration where modes A_0 and B_0 are coupled. Configurations where other pairs of modes are coupled can be treated in a similar manner. For an asymmetric filter one has to consider separately both the coupling of modes A_0, B_1 and A_1, B_0 because the symmetry is broken.

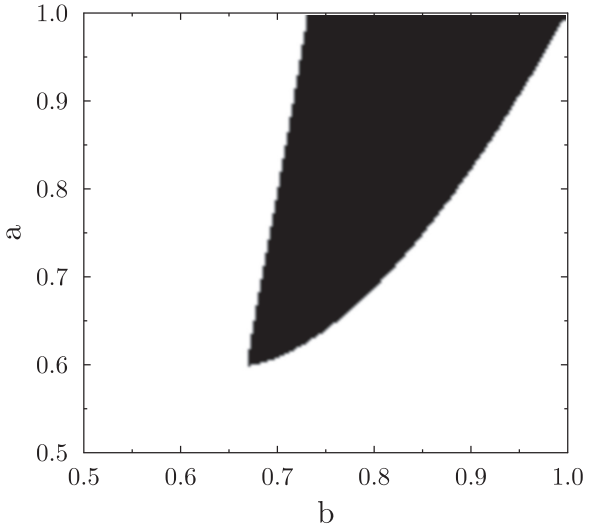

FIG. 4. The black area indicates the range of parameters a and b of a symmetric two-qubit quantum filter (9) for which the coupling of modes B_0 and A_1 leads to maximum success probability P_L.

A. Asymmetric real filter

Let us consider the linear-optical implementation of an asymmetric real filter

$$M = a|00\rangle\langle 00| + b_A|01\rangle\langle 01| + b_B|10\rangle\langle 10| + |11\rangle\langle 11|, \quad (52)$$

where $0 \leqslant a \leqslant 1$, and $0 \leqslant b_A \leqslant b_B \leqslant 1$ are real parameters of the filter. Assuming the coupling of modes A_0 and B_0, the matrix U_{AB} can be conveniently parametrized as

$$U_{AB} = \begin{pmatrix} b_A\tau_A & b_A\tau_A x & 0 & 0 \\ b_B\tau_B y & b_B\tau_B & 0 & 0 \\ 0 & 0 & \tau_A & 0 \\ 0 & 0 & 0 & \tau_B \end{pmatrix}, \quad (53)$$

where

$$xy = \frac{a}{b^2} - 1, \quad (54)$$

and we have defined the parameter $b = \sqrt{b_A b_B}$. Since U_{AB} is a submatrix of a unitary matrix, the following inequalities must hold, similarly to the previously studied case of a symmetric filter,

$$\tau_A^2 \leqslant 1, \quad \tau_B^2 \leqslant 1, \quad (55)$$

$$b_A^2\tau_A^2(1+x^2) \leqslant 1, \quad b_B^2\tau_B^2(1+y^2) \leqslant 1, \quad (56)$$

and

$$\eta_A^2\eta_B^2(x+y)^2 \leqslant \big[1-\eta_A^2(1+x^2)\big]\big[1-\eta_B^2(1+y^2)\big], \quad (57)$$

where $\eta_A = b_A\tau_A$ and $\eta_B = b_B\tau_B$. With the use of condition (54), the last inequality can be rewritten as

$$\eta_A^2(1+x^2) + \eta_B^2(1+y^2) - \eta_A^2\eta_B^2\Big(2 - \frac{a}{b^2}\Big)^2 \leqslant 1. \quad (58)$$

For any filter (52), the optimal interferometer maximizing $P_L = \tau_A^2\tau_B^2$ can always be designed such that the inequality (58) is saturated and equality holds. First note that if one of the inequalities (56) is saturated, then also inequality (57) is saturated and equality must hold, because both the left- and right-handed sides of Eq. (57) must be equal to 0. Assume now a configuration where none of the inequalities (56) and (57) is saturated. If τ_A or τ_B is smaller than 1, then we can increase their value until either equality holds in (57) or $\tau_A = \tau_B = 1$. For an optimal configuration with $\tau_A = \tau_B = 1$ we can increase or decrease the free parameter x while keeping the constraint (54) until the equality holds in Eq. (57).

We now discuss the various options that have to be considered. Let us first consider the option $\tau_A = \tau_B = 1$, i.e., $P_L = 1$. In this case, x and y can be determined by solving Eqs. (54) and (58), where the equality is assumed to hold. We obtain

$$x^2 = \frac{1}{2b_A^2}\big[q + \sqrt{q^2 - 4(a-b^2)^2}\big],$$
$$y^2 = \frac{1}{2b_B^2}\big[q - \sqrt{q^2 - 4(a-b^2)^2}\big], \quad (59)$$

where

$$q = 1 - b_A^2 - b_B^2 + (2b^2 - a)^2. \quad (60)$$

Since x^2 and y^2 must be real and non-negative, the solution (59) exists only if

$$q \geqslant 2|a - b^2|. \tag{61}$$

Additionally, the inequalities (56) must also hold, which reduces to

$$x^2 \leqslant \frac{1}{b_A^2} - 1, \quad y^2 \leqslant \frac{1}{b_B^2} - 1, \tag{62}$$

where x^2 and y^2 are given by Eq. (59). To sum up, $P_L = 1$ is achievable with the coupling of modes A_0 and B_0 if and only if the inequalities (61) and (62) are satisfied.

Let us now assume that $\tau_A = 1$ but τ_B can be smaller than 1. Assuming equality in Eq. (58), we get

$$\tau_B^2 = \frac{b_A^2 x^2\left[1 - b_A^2(1 + x^2)\right]}{b^4 x^2 + (a - b^2)^2 - b_A^2 x^2 (2b^2 - a)^2}. \tag{63}$$

The optimal x^2 that maximizes τ_B^2 can be determined by solving the extremal equation

$$\frac{\partial \tau_B^2}{\partial x} = 0. \tag{64}$$

This leads to a quadratic equation for x^2 with roots

$$\begin{aligned} x^2 &= \frac{(a - b^2)(1 - b_A)}{b_A(b^2 + ab_A - 2b^2 b_A)}, \\ x^2 &= \frac{(b^2 - a)(1 + b_A)}{b_A(b^2 - ab_A + 2b^2 b_A)}. \end{aligned} \tag{65}$$

These roots represent valid solutions provided that $x^2 \geqslant 0$ and the inequalities (55) and (56) are satisfied, where y^2 and τ_B^2 are determined by Eqs. (54) and (63), respectively. For an asymmetric filter we must also independently consider the configuration $\tau_B = 1$ because the symmetry is broken. Following a similar procedure as before, we obtain

$$\tau_A^2 = \frac{b_B^2 y^2\left[1 - b_B^2(1 + y^2)\right]}{b^4 y^2 + (a - b^2)^2 - b_B^2 y^2 (2b^2 - a)^2}, \tag{66}$$

and the potentially optimal y^2 read

$$\begin{aligned} y^2 &= \frac{(a - b^2)(1 - b_B)}{b_B(b^2 + ab_B - 2b^2 b_B)}, \\ y^2 &= \frac{(b^2 - a)(1 + b_B)}{b_B(b^2 - ab_B + 2b^2 b_B)}. \end{aligned} \tag{67}$$

Once again these solutions are valid only if $y^2 \geqslant 0$ and the inequalities (55) and (56) are satisfied.

Finally, we consider the configuration where both τ_A and τ_B can be smaller than 1. Assuming equality in (58), we can express τ_A as a function of τ_B and x,

$$\tau_A^2 = \frac{b_B^2 y^2\left[1 - b_B^2 \tau_B^2(1 + y^2)\right]}{b^4 y^2 + (a - b^2)^2 - b_B^2 \tau_B^2 y^2 (2b^2 - a)^2}. \tag{68}$$

On inserting this formula into the extremal equations

$$\frac{\partial}{\partial \tau_B}\left(\tau_A^2 \tau_B^2\right) = 0, \quad \frac{\partial}{\partial y}\left(\tau_A^2 \tau_B^2\right) = 0, \tag{69}$$

we obtain after some algebra the following expressions for x and y,

$$x = \frac{\sqrt{|a - b^2|}}{b}, \quad y = \operatorname{sgn}(a - b^2)\frac{\sqrt{|a - b^2|}}{b}. \tag{70}$$

If $a \leqslant b^2$, then $x = -y$ and at least one of the inequalities (56) is saturated. However, the inequalities (55) may represent an additional bound. We can succinctly express τ_A and τ_B as follows,

$$\begin{aligned} \tau_A^2 &= \min\left(1, \frac{b^2}{b_A^2(2b^2 - a)}\right), \\ \tau_B^2 &= \min\left(1, \frac{b^2}{b_B^2(2b^2 - a)}\right). \end{aligned} \tag{71}$$

If $a > b^2$, then the extremal equations (69) lead to the following expressions for τ_A and τ_B,

$$\tau_A^2 = \frac{b_B}{b_A}\frac{1}{(\sqrt{a - b^2} + b)^2}, \quad \tau_B^2 = \frac{b_A}{b_B}\frac{1}{(\sqrt{a - b^2} + b)^2}. \tag{72}$$

These formulas represent valid solutions only if the inequalities (55) and (56) are satisfied.

B. Symmetric complex filter

Let us finally investigate the realization of symmetric two-qubit filters with complex coefficients. Without loss of generality, we can restrict ourselves to the filters

$$M = ae^{i\varphi}|00\rangle\langle 00| + b|01\rangle\langle 01| + b|10\rangle\langle 10| + |11\rangle\langle 11|, \tag{73}$$

where a and b are real and positive, because the relative phase shifts of states $|01\rangle$ and $|10\rangle$ can be set to zero by suitable phase shifts applied to modes A_0 and B_0, respectively. We shall again focus on the configuration where modes A_0 and B_0 are coupled. The matrix U_{AB} has the same structure as for real symmetric filters,

$$U_{AB} = \begin{pmatrix} b\tau_A & \tau_A x & 0 & 0 \\ \tau_B y & b\tau_B & 0 & 0 \\ 0 & 0 & \tau_A & 0 \\ 0 & 0 & 0 & \tau_B \end{pmatrix}, \tag{74}$$

only the condition on parameters x and y changes to

$$xy = ae^{i\varphi} - b^2. \tag{75}$$

Since x and y are generally complex, the conditions implied by U_{AB} being a submatrix of a unitary matrix must be written as follows,

$$\tau_A^2(b^2 + |x|^2) \leqslant 1, \quad \tau_B^2(b^2 + |y|^2) \leqslant 1, \tag{76}$$

and

$$b^2\tau_A^2\tau_B^2|x + y^*|^2 \leqslant \left[1 - \tau_A^2(b^2 + |x|^2)\right]\left[1 - \tau_B^2(b^2 + |y|^2)\right]. \tag{77}$$

Taking into account the symmetry of the filter, one can show that $P_L = 1$ can be achieved provided that the inequalities (76) and (77) are satisfied for a symmetric configuration with $|x| = |y|$ and $\tau_A = \tau_B = 1$. After some algebra, this yields the following condition,

$$b^2 + b\sqrt{2(s + a\cos\varphi - b^2)} + s \leqslant 1, \tag{78}$$

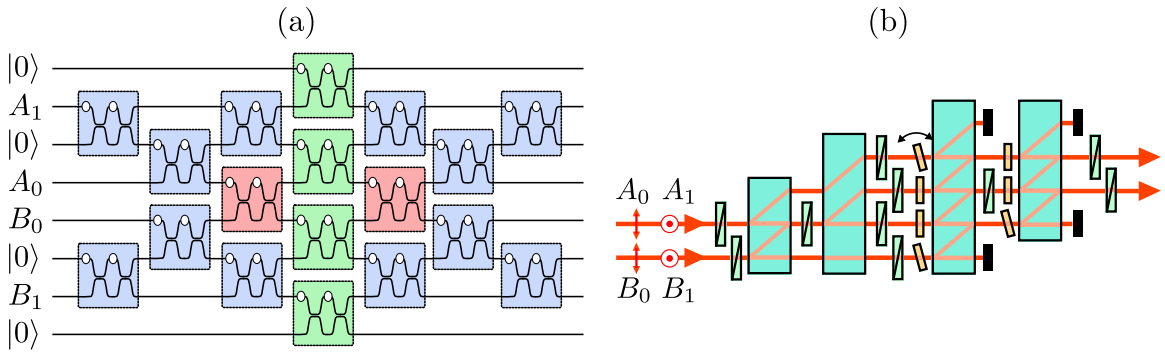

FIG. 5. Two examples of a possible implementation of the two-qubit linear-optical quantum filters. (a) On-chip implementation with path encoding of the qubit states. Lines represent the optical waveguides and their crossings balanced directional couplers. The open circles indicate variable phase shifters. Subblocks in colored boxes act as variable beam splitters. Blue boxes serve for mode swapping that ensures coupling of the desired pair of modes. The two red boxes realize the required interferometric coupling of the selected pair of signal carrying modes, and the four green boxes serve for tunable signal attenuation in each mode. (b) Bulk-optics implementation with polarization encoding and interferometers formed by calcite beam displacers that introduce a lateral shift between the vertically and horizontally polarized beams. The polarization states are transformed with half-wave plates (green elements) that play the role of beam splitters, and the interferometric phase shifts can be set and controlled by tilting thin glass plates (orange elements).

where

$$s = |xy| = \sqrt{a^2 + b^4 - 2ab^2\cos\varphi}. \tag{79}$$

If the inequality (78) does not hold, then the optimal configuration is symmetric, with

$$x = y = \sqrt{ae^{i\varphi} - b^2}, \tag{80}$$

and

$$\tau_A^2 = \tau_B^2 = \frac{1}{b^2 + b\sqrt{2(s + a\cos\varphi - b^2)} + s}. \tag{81}$$

This yields

$$P_L = \left[b^2 + b\sqrt{2(s + a\cos\varphi - b^2)} + s\right]^{-2}. \tag{82}$$

For $\varphi = 0$ we recover the results for a symmetric real filter derived in Sec. III A. Also, for $a = b = 1$ we recover from Eq. (82) the maximum probability of implementation of a two-qubit linear-optical controlled-phase gate [33,34],

$$P_{\rm CP}(\varphi) = \left[1 + 2\left|\sin\frac{\varphi}{2}\right| + 2\sqrt{\left|\sin\frac{\varphi}{2}\right| - \sin^2\frac{\varphi}{2}}\right]^{-2}. \tag{83}$$

We note that also for $\varphi = \pi$ we obtain a filter (9) with real parameters a and b, where the effective coefficient a becomes negative. The results obtained in Secs. III and IV A for real symmetric and asymmetric quantum filters are straightforwardly applicable also if $a < 0$, and one only needs to carefully check whether a given potentially optimal solution is meaningful for $a < 0$. Recall that a filter with negative b_A or b_B can be converted to a filter with positive b_A and b_B by single-mode unitary phase shifts. Therefore, it suffices to allow for negative a to cover the whole class of real filters. A real filter with $a < 0$ can be seen as a combination of a filter with positive real coefficients and a unitary controlled-Z gate.

V. CONCLUSIONS

We have designed optimal interferometric schemes for the implementation of two-qubit linear-optical quantum filters operating in the coincidence basis. The considered linear-optical realization of the quantum filters may impose an extra cost in terms of a reduced success probability of successful filtering and the designed schemes maximize the success probability of the filter. The symmetric real filters were analyzed in particular detail and, interestingly, we have found that for a certain range of parameters the optimal scheme is asymmetric in the sense that it couples a pair of modes corresponding to logical state $|1\rangle$ of one qubit and logical state $|0\rangle$ of the other qubit, which contrasts the symmetry of the considered filter. Our investigation of the optimal implementation of optical quantum filters complements the earlier studies on the optimal realization of linear-optical unitary quantum gates. The required interferometric setup can be implemented on-chip with integrated optics where a tunable beam splitter can be realized using a Mach-Zehnder interferometer with a tunable phase shift [6,39,40]. A universal integrated optics circuit that can realize all of the optimal interferometric schemes is drawn in Fig. 5(a). As a second example, in Fig. 5(b) we show a possible bulk optics realization based on polarization qubit encoding and the utilization of inherently stable interferometers formed by a sequence of calcite beam displacers [11,41–43]. The investigated two-qubit linear-optical quantum filters may find applications in linear-optics quantum information processing and quantum state engineering.

ACKNOWLEDGMENT

We acknowledge support by the Czech Science Foundation under Grant No. 19-19189S.

APPENDIX: DERIVATION OF THE STRUCTURE OF MATRIX U_{AB}

In this Appendix we determine the most general form of the 4×4 matrix $U_{j,k}$, $j,k \in A_0, B_0, A_1, B_1$, that describes interferometric coupling which enables the implementation of the diagonal two-qubit quantum filter (9). Recall that the input

two-photon Fock state $|\mathbf{1}_{A_j}, \mathbf{1}_{B_k}\rangle$ transforms as follows,

$$|\mathbf{1}_{A_j}, \mathbf{1}_{B_k}\rangle \rightarrow \sum_{m,n=0}^{1} \left(U_{A_j,A_m}U_{B_k,B_n} + U_{A_j,B_n}U_{B_k,A_m}\right)|\mathbf{1}_{A_m}, \mathbf{1}_{B_n}\rangle, \tag{A1}$$

where we assume operation in the coincidence basis and restrict ourselves to the outputs where a single photon is present in each pair of modes A_0, A_1 and B_0, B_1. Recall also that the implementation of a diagonal two-qubit quantum filter $M = \sum_{j,k=0}^{1} m_{jk}|jk\rangle\langle jk|$ requires that

$$U_{A_j,A_m}U_{B_k,B_n} + U_{A_j,B_n}U_{B_k,A_m} = \sqrt{P_L}m_{jk}\delta_{jm}\delta_{kn}. \tag{A2}$$

Throughout the following discussion we assume that all four coefficients m_{jk} are nonzero. Let us first prove that all four diagonal matrix elements U_{A_j,A_j} and U_{B_k,B_k} must be nonzero. Assume that $U_{A_0,A_0} = 0$. In order to obtain nonzero m_{A_0,B_0} and m_{A_0,B_1} the matrix elements U_{B_0,A_0}, U_{A_0,B_0}, U_{A_0,B_1}, and U_{B_1,A_0} must be all nonzero. However, this implies that

$$U_{A_0,A_0}U_{B_0,B_1} + U_{A_0,B_1}U_{B_0,A_0} \tag{A3}$$

is nonzero, which is in contradiction with the required structure (A2). Specifically, the nonzero term (A3) implies that the input state $|\mathbf{1}_{A_0}, \mathbf{1}_{B_0}\rangle$ is transformed to a state that contains a nonvanishing contribution of $|\mathbf{1}_{A_0}, \mathbf{1}_{B_1}\rangle$, which is not compatible with the diagonal form of the targeted quantum filter. We have thus proved by contradiction that U_{A_0,A_0} must be nonzero. The same proof applies also to the other three matrix elements U_{A_1,A_1}, U_{B_0,B_0}, and U_{B_1,B_1}.

We next show that the four matrix elements U_{A_0,A_1}, U_{A_1,A_0}, U_{B_0,B_1}, and U_{B_1,B_0} must be zero. We again prove this by contradiction. We provide the proof for U_{A_0,A_1}. Equation (A2) implies that

$$\begin{aligned} U_{A_0,A_0}U_{B_0,B_1} &= -U_{A_0,B_1}U_{B_0,A_0}, \\ U_{A_0,A_1}U_{B_0,B_0} &= -U_{A_0,B_0}U_{B_0,A_1}, \\ U_{A_0,A_1}U_{B_0,B_1} &= -U_{A_0,B_1}U_{B_0,A_1}. \end{aligned} \tag{A4}$$

If we take the product of the first two equations (A4) and make use of the third equality (A4), we obtain

$$U_{A_0,A_1}U_{B_0,B_1}\left(U_{A_0,A_0}U_{B_0,B_0} + U_{A_0,B_0}U_{B_0,A_0}\right) = 0. \tag{A5}$$

Since the term in the parentheses is equal to $\sqrt{P_L}m_{00}$ and thus nonzero, we have

$$U_{A_0,A_1}U_{B_0,B_1} = 0. \tag{A6}$$

This implies that also

$$U_{A_0,B_1}U_{B_0,A_1} = 0. \tag{A7}$$

If $U_{A_0,A_1} \neq 0$, then also $U_{B_0,A_1} \neq 0$, and $U_{A_0,B_1} = 0$, which follows from Eqs. (A4) and (A6) and from the above proved condition $U_{B_0,B_0} \neq 0$. It follows that the amplitude

$$U_{A_0,A_1}U_{B_1,B_1} + U_{A_0,B_1}U_{B_1,A_1} \tag{A8}$$

is nonzero, although it should vanish. Therefore, $U_{A_0,A_1} = 0$ must hold and similarly we can show that also $U_{A_1,A_0} = U_{B_0,B_1} = U_{B_1,B_0} = 0$.

Let us now assume that modes A_0 and B_0 are interferometrically coupled and $U_{A_0,B_0} \neq 0$, as well as $U_{B_0,A_0} \neq 0$. We show that the other pairs of modes A_j and B_k cannot be coupled. It follows immediately from Eq. (A4) that

$$U_{A_0,B_1} = U_{B_0,A_1} = 0. \tag{A9}$$

We next consider the following amplitudes that should also vanish,

$$\begin{aligned} U_{B_1,B_0}U_{A_0,A_0} + U_{A_0,B_0}U_{B_1,A_0} = 0, \\ U_{A_1,A_0}U_{B_0,B_0} + U_{A_1,B_0}U_{B_0,A_0} = 0, \end{aligned} \tag{A10}$$

Since $U_{B_1,B_0} = U_{A_1,A_0} = 0$ and $U_{A_0,B_0} \neq 0$, $U_{B_0,A_0} \neq 0$, we get

$$U_{A_1,B_0} = U_{B_1,A_0} = 0. \tag{A11}$$

Finally, from the requirement that the following two amplitudes should vanish,

$$\begin{aligned} U_{A_1,B_1}U_{B_0,A_0} + U_{A_1,A_0}U_{B_0,B_1} = 0, \\ U_{B_1,A_1}U_{A_0,B_0} + U_{A_0,A_1}U_{B_1,B_0} = 0, \end{aligned} \tag{A12}$$

we can deduce that

$$U_{A_1,B_1} = U_{B_1,A_1} = 0. \tag{A13}$$

To summarize our findings: Out of the 16 matrix elements $U_{j,k}$, where $j, k \in \{A_0, A_1, B_0, B_1\}$, only six elements are nonzero, the four diagonal elements $U_{j,j}$ and two elements representing interferometric coupling of a single pair of modes A_j and B_k, e.g., U_{A_0,B_0} and U_{B_0,A_0}. The matrix (10) considered in Sec. III A of the main text (or its variants obtained by swapping the modes A_0 and A_1 and/or B_0 and B_1) therefore represents the most general permissible interferometric coupling for the implementation of two-qubit diagonal quantum filters.

We note that, strictly speaking, this result holds only if all four m_{jk} are nonzero. If two or three filter parameters m_{jk} vanish, then it can be shown that the filter can be implemented with $P_L = 1$ and the coupling of one pair of modes is sufficient to achieve this. In fact, the only nontrivial configuration is $m_{01} = m_{10} = 0$ while $m_{00} \neq 0$, and this is covered by the optimal symmetric quantum filters discussed in Sec. III. Otherwise, $m_{00} = m_{01}m_{10}$ holds, and the filter factorizes into a product of two single-qubit filters. For the remaining case of one vanishing parameter one can conjecture that the dependence of P_L on the filter parameters should be continuous and therefore it should suffice to consider the above identified interferometric configurations with one pair of coupled modes.

[1] P. Kok and B. W. Lovett, *Introduction to Optical Quantum Information Processing* (Cambridge University Press, Cambridge, UK, 2014).

[2] S. Slussarenko and G. J. Pryde, Appl. Phys. Rev. **6**, 041303 (2019).

[3] F. Flamini, N. Spagnolo, and F. Sciarrino, Rep. Prog. Phys. **82**, 016001 (2019).

[4] E. Knill, R. Laflamme, and G. J. Milburn, Nature (London) **409**, 46 (2001).

[5] P. Kok, W. J. Munro, K. Nemoto, T. C. Ralph, J. P. Dowling, and G. J. Milburn, Rev. Mod. Phys. **79**, 135 (2007).

[6] J. Wang, F. Sciarrino, A. Laing, and M. G. Thompson, Nat. Photon. **14**, 273 (2020).

[7] F. Marsili, V. B. Verma, J. A. Stern, S. Harrington, A. E. Lita, T. Gerrits, I. Vayshenker, B. Baek, M. D. Shaw, R. P. Mirin *et al.*, Nat. Photon. **7**, 210 (2013).

[8] H. Le Jeannic, V. B. Verma, A. Cavaillès, F. Marsili, M. D. Shaw, K. Huang, O. Morin, S. W. Nam, and J. Laurat, Opt. Lett. **41**, 5341 (2016).

[9] P. Senellart, G. Solomon, and A. White, Nat. Nanotechnol. **12**, 1026 (2017).

[10] E. Meyer-Scott, C. Silberhorn, and A. Migdall, Rev. Sci. Instrum. **91**, 041101 (2020).

[11] B. P. Lanyon, M. Barbieri, M. P. Almeida, T. Jennewein, T. C. Ralph, K. J. Resch, G. J. Pryde, J. L. O'Brien, A. Gilchrist, and A. G. White, Nat. Phys. **5**, 134 (2009).

[12] M. Mičuda, M. Sedlák, I. Straka, M. Miková, M. Dušek, M. Ježek, and J. Fiurášek, Phys. Rev. Lett. **111**, 160407 (2013).

[13] R. B. Patel, J. Ho, F. Ferreyrol, T. C. Ralph, and G. J. Pryde, Sci. Adv. **2**, e1501531 (2016).

[14] T. Ono, R. Okamoto, M. Tanida, H. F. Hofmann, and S. Takeuchi, Sci. Rep. **7**, 45353 (2017).

[15] R. Stárek, M. Mičuda, M. Miková, I. Straka, M. Dušek, P. Marek, M. Ježek, R. Filip, and J. Fiurášek, npj Quantum Inf. **4**, 35 (2018).

[16] B. Huttner, A. Muller, J. D. Gautier, H. Zbinden, and N. Gisin, Phys. Rev. A **54**, 3783 (1996).

[17] R. B. M. Clarke, A. Chefles, S. M. Barnett, and E. Riis, Phys. Rev. A **63**, 040305(R) (2001).

[18] C. H. Bennett, H. J. Bernstein, S. Popescu, and B. Schumacher, Phys. Rev. A **53**, 2046 (1996).

[19] P. G. Kwiat, S. Barraza-Lopez, A. Stefanov, and N. Gisin, Nature (London) **409**, 1014 (2001).

[20] H. Takahashi, J. S. Neergaard-Nielsen, M. Takeuchi, M. Takeoka, K. Hayasaka, A. Furusawa, and M. Sasaki, Nat. Photon. **4**, 178 (2010).

[21] Y. Kurochkin, A. S. Prasad, and A. I. Lvovsky, Phys. Rev. Lett. **112**, 070402 (2014).

[22] A. Zavatta, S. Viciani, and M. Bellini, Science **306**, 660 (2004).

[23] J. Wenger, R. Tualle-Brouri, and P. Grangier, Phys. Rev. Lett. **92**, 153601 (2004).

[24] A. Ourjoumtsev, R. Tualle-Brouri, J. Laurat, and P. Grangier, Science **312**, 83 (2006).

[25] R. Kumar, E. Barrios, C. Kupchak, and A. I. Lvovsky, Phys. Rev. Lett. **110**, 130403 (2013).

[26] A. I. Lvovsky, P. Grangier A. Ourjoumtsev, V. Parigi, M. Sasaki, and R. Tualle-Brouri, arXiv:2006.16985.

[27] T. B. Pittman, B. C. Jacobs, and J. D. Franson, Phys. Rev. Lett. **88**, 257902 (2002).

[28] T. B. Pittman, B. C. Jacobs, and J. D. Franson, Phys. Rev. A **64**, 062311 (2001).

[29] H. F. Hofmann and S. Takeuchi, Phys. Rev. Lett. **88**, 147901 (2002).

[30] S. Gasparoni, J.-W. Pan, P. Walther, T. Rudolph, and A. Zeilinger, Phys. Rev. Lett. **93**, 020504 (2004).

[31] Z. Zhao, A.-N. Zhang, Y.-A. Chen, H. Zhang, J.-F. Du, T. Yang, and J.-W. Pan, Phys. Rev. Lett. **94**, 030501 (2005).

[32] D. E. Browne and T. Rudolph, Phys. Rev. Lett. **95**, 010501 (2005).

[33] K. Kieling, J. L. O'Brien, and J. Eisert, New J. Phys. **12**, 013003 (2010).

[34] K. Lemr, A. Černoch, J. Soubusta, K. Kieling, J. Eisert, and M. Dušek, Phys. Rev. Lett. **106**, 013602 (2011).

[35] R. Okamoto, H. F. Hofmann, S. Takeuchi, and K. Sasaki, Phys. Rev. Lett. **95**, 210506 (2005).

[36] N. K. Langford, T. J. Weinhold, R. Prevedel, K. J. Resch, A. Gilchrist, J. L. O'Brien, G. J. Pryde, and A. G. White, Phys. Rev. Lett. **95**, 210504 (2005).

[37] N. Kiesel, C. Schmid, U. Weber, R. Ursin, and H. Weinfurter, Phys. Rev. Lett. **95**, 210505 (2005).

[38] P. Kok, H. Lee, and J. P. Dowling, Phys. Rev. A **66**, 063814 (2002).

[39] J. Carolan, C. Harrold, C. Sparrow, E. Martín-López, N. J. Russell, J. W. Silverstone, P. J. Shadbolt, N. Matsuda, M. Oguma, M. Itoh, G. D. Marshall, M. G. Thompson, J. C. F. Matthews, T. Hashimoto, J. L. O'Brien, and A. Laing, Science **14**, 711 (2015).

[40] X. Qiang X. Zhou, J. Wang, C. M. Wilkes, T. Loke, S. O'Gara, L. Kling, G. D. Marshall, R. Santagati, T. C. Ralph, J. B. Wang, J. L. O'Brien, M. G. Thompson, and J. C. F. Matthews, Nat. Photon. **12**, 534 (2018).

[41] M. A. Broome, A. Fedrizzi, B. P. Lanyon, I. Kassal, A. Aspuru-Guzik, and A. G. White, Phys. Rev. Lett. **104**, 153602 (2010).

[42] Z.-H. Bian, J. Li, X. Zhan, J. Twamley, and P. Xue, Phys. Rev. A **95**, 052338 (2017).

[43] R. Stárek, M. Miková, I. Straka, M. Dušek, M. Ježek, J. Fiurášek, and M. Mičuda, Opt. Express **26**, 8443 (2018).